AIP | Applied Physics Letters

Plasmon-enhanced internal photoemission for photovoltaics: Theoretical efficiency limits

Thomas P. White and Kylie R. Catchpole

Citation: Appl. Phys. Lett. **101**, 073905 (2012); doi: 10.1063/1.4746425
View online: http://dx.doi.org/10.1063/1.4746425
View Table of Contents: http://apl.aip.org/resource/1/APPLAB/v101/i7
Published by the American Institute of Physics.

Plasmon-enhanced internal photoemission for photovoltaics: Theoretical efficiency limits

Thomas P. White[a] and Kylie R. Catchpole
Centre for Sustainable Energy Systems, Research School of Engineering, The Australian National University, Canberra, Australian Capital Territory, Australia

(Received 10 July 2012; accepted 2 August 2012; published online 17 August 2012)

Plasmon-enhanced internal photoemission in metal-semiconductor Schottky junctions has recently been proposed as an alternative photocurrent mechanism for solar cells. Here, we identify and discuss the requirements for efficient operation of such cells and analyze their performance limits under standard solar illumination. We show that the maximum efficiency limit is <8% even if perfect optical absorption can be achieved using plasmonic nanostructures. This limit results from the fundamental electronic properties of metallic absorbers. Modifying the electron density of states of the absorber could increase the efficiency to >20%. © *2012 American Institute of Physics*. [http://dx.doi.org/10.1063/1.4746425]

Global efforts to reduce the cost of photovoltaic (PV) electricity are driving interest in alternative solar cell geometries and light absorption mechanisms. Plasmonic nanostructures have been used to increase absorption in thin-film solar cells through efficient scattering and trapping of incident light in the semiconductor absorber.[1] An alternative use of plasmonic enhancement for PV has been proposed, whereby photons are absorbed directly in the metal, generating "hot" energetic electrons (or holes), that can then be extracted from the metal via internal photoemission (IPE) across a metal-semiconductor Schottky junction[2–5] (see Fig. 1). This photocurrent mechanism is used in infra-red photodetectors, but efficiencies are typically low, in part due to weak absorption of light in the metal.[6] However, recent progress on plasmonic absorption enhancement has seen a renewed interest in IPE, and its application in photovoltaics.[2–5]

Several experimental demonstrations of plasmon-enhanced IPE have been reported, but quantum efficiencies remain relatively low. Incident photon-to-current conversion efficiencies (IPCEs) (or external quantum efficiencies (EQEs)) up to 8.4% were reported for Au nanoparticles on TiO_2 in a cell that included a liquid hole transport layer,[2] while solid-state versions typically have IPCE <2.5%.[3,7] No experimental power conversion efficiencies have been reported for standard solar illumination; however, theoretical efficiencies of ~4% were calculated for one specific cell geometry combining plasmonic absorption and IPE.[4]

Given the recent interest in IPE for PV applications, it is important to identify the efficiency limits of this process for energy conversion. Here, we discuss the key optical and electronic processes in such cells and their influence on IPCE and overall cell efficiency. We show that even with perfect optical absorption and efficient emission of hot electrons into the semiconductor, the maximum possible power conversion efficiency is <8%, using realistic materials. This limit is a direct consequence of the metallic absorber, in which the high density of unoccupied energy levels above the Fermi level results in a broad distribution of hot electron energies, many of which have insufficient energy to be emitted into the semiconductor. While the results are discouraging for the future of plasmon enhanced IPE solar cells, they highlight specific areas for further research that may lead to increased efficiency limits beyond those presented here.

Figure 1(a) shows the basic cell geometry consisting of a metal nanoparticle absorber on a semiconductor surface. The metal-semiconductor interface forms a Schottky junction characterized by a barrier of height Φ_B (Fig. 1(c)). The junction is shown here for an n-type semiconductor, but our discussion also applies to p-type semiconductors, in which case holes would be emitted across the junction. In theory, the barrier height depends only on the work functions of the metal and the semiconductor, but in practice the details of the interface layers play a strong role. This gives IPE devices significant flexibility in the choice of semiconductor, since the photocurrent response depends more the junction properties than on the semiconductor bandgap. The different energy levels on either side of the junction allow hot electrons with sufficient kinetic energy to be emitted from the metal into the conduction band of the semiconductor, while providing a barrier to conduction band electrons crossing the interface in the opposite direction. When exposed to light, this

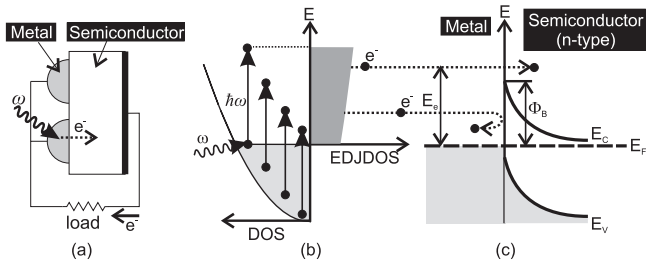

FIG. 1. (a) Geometry of a plasmon-enhanced internal photoemission solar cell. (b) Excitation of electrons in the metal from occupied energy levels in the conduction band (shaded gray) to unoccupied levels above the Fermi energy E_F. Left axis: parabolic density of states (DOS) in the conduction band. Right axis: distribution of hot electron energies given by the EDJDOS. (c) Energy diagram of the Schottky junction at the metal-semiconductor interface (shown for an n-type semiconductor). Hot electrons with energy $>\Phi_B$ can be emitted over the barrier into the semiconductor; those without enough energy are reflected back into the metal.

[a]Electronic mail: thomas.white@anu.edu.au.

asymmetry produces a voltage across the cell that can drive a photocurrent through an external circuit.

Photocurrent generation involves (i) absorption of photons in the metal, and generation of hot electrons; (ii) ballistic transport of the hot electrons through the metal to the interface; (iii) emission of the electron across the junction; and (iv) collection of the electrons at a contact. Electrons then pass through the external load and are returned to the metal either via a (solid or liquid) hole-conducting layer[2,3,5] or directly.[7] Here, we assume that all electrons emitted at step (iii) are collected in step (iv). This is reasonable since electrons are majority carriers in the semiconductor, so bulk recombination losses will be low. Hence, we will not discuss step (iv) further. Instead, we focus on the key features of steps (i)-(iii) that determine the efficiency of IPE solar cells.

The current density response of the cell can be approximated by the equation[8]

$$j_{\text{cell}} = j_{\text{sc}} - A^* T^2 e^{-\Phi_B/kT}(e^{V/kT} - 1), \tag{1}$$

where j_{sc} is the short circuit photocurrent density, and the second term on the right is the reverse current due to thermionic emission over the Schottky barrier. This second term is the standard Schottky diode equation, where the term A^* is the modified Richardson constant, k is the Boltzmann constant, T is the temperature, and V is the voltage across the cell. The total short circuit current density can be written as

$$j_{\text{sc}} = q\int \varphi(\lambda)\eta_{abs}(\lambda)\eta_i(\lambda)d\lambda, \tag{2}$$

where q is the charge on an electron, $\varphi(\lambda)$ is the incident photon flux, $\eta_{abs}(\lambda)$ is the optical absorption in the metal, and η_i is the electron emission efficiency, which includes both transport through the metal and emission over the Schottky barrier.

In the absence of plasmonic effects, photons incident on a metal surface may be absorbed directly, exciting electrons from occupied energy levels below the Fermi energy into unoccupied energy levels in the conduction band (Fig. 1(b)). Planar metal surfaces typically have a high reflectance so direct optical absorption tends to be low. Structuring the metal layer to support surface plasmon resonances can increase the optical absorption, and thus the generated photocurrent.[3,5,7] Once excited on a metal surface, plasmons lose energy via radiative damping (re-emission of light, or scattering) and non-radiative damping (generation of electron-hole pairs).[9] Efficient plasmonic absorption occurs when non-radiative damping dominates, as is the case for small plasmonic nanoparticles (a few tens of nm in size) or appropriately designed surfaces. These structures can exhibit strong broadband, polarization insensitive, absorption,[10] and would thus be well-suited for IPE devices. Here, we treat the metal as an ideal optical absorber across the solar spectrum ($\eta_{abs} = 1$), and thus the calculated efficiencies should be treated as absolute upper limits.

Immediately after a photon has been absorbed, the excited electron will have an energy E_e above the Fermi distribution of the surrounding electrons, as illustrated in Fig. 1(b). This hot electron may have enough energy to cross the Schottky barrier, but this must occur before the excess energy is lost to nearby electrons or atoms. An electron in the conduction band of the metal may be excited from an initial energy E_i in the range $E_F - \hbar\omega < E_i < E_F$, to an energy $E_F + E_e$, where $0 < E_e < \hbar\omega$, $\hbar\omega$ is the photon energy, and E_e is the excess kinetic energy above the Fermi level.[11] The distribution of final electron energies depends on the probability of each electron transition occurring. It is common in the literature to assign an equal probability to all permitted transitions, resulting in a uniform electron energy distribution[4,11] in the range $0 < E_e < \hbar\omega$. While this is valid for intraband transitions in many noble metals when $\hbar\omega \gg kT$, here we take a more general approach based on electron density of states (DOS) that allows us to identify potential strategies to improve the efficiency of IPE.

The distribution of hot electron energies is described by the electron distribution joint density of states (EDJDOS),[12–14] illustrated schematically in Fig. 1(b). Rigorous EDJDOS calculations are required for high energy photons that may interact with multiple energy bands well below E_F, and include electron bandstructure and momentum conservation rules. Here, we are interested in solar spectrum wavelengths, and thus photon energies of $\hbar\omega < 3\,\text{eV}$, so we instead apply a simplified expression for the EDJDOS ($\mathcal{D}$) given by the product of the electron DOS at the initial and final electron energies,[13,14]

$$\mathcal{D}(E, \hbar\omega) = \rho(E - \hbar\omega)\rho(E), \tag{3}$$

where E is the energy of the excited electron, $\hbar\omega$ is the photon energy, $E - \hbar\omega$ is the initial electron energy, and $\rho(E)$ is the electron DOS. This non-direct approximation assumes that conservation of electron momentum is unimportant and has been shown to agree well with experimental photoemission measurements for a range of noble metals.[13] In these metals, the conduction band density of states is well approximated by the free electron gas model, where $\rho \propto E^{1/2}$ with the energy measured from the bottom of the conduction band.

Figure 2(a) shows EDJDOS curves calculated using Eq. (3) for a metal with the Fermi level 5.5 eV above the bottom of the conduction band. This is a good approximation for Au and Ag, provided the photon energy is low enough to avoid interband transitions from the d-band energy levels which lie 2.4 eV and 4 eV below E_F for Au and Ag, respectively.[16] The three curves in Fig. 2(a) show the EDJDOS for incident photon energies of 1.3 eV ($\lambda = 954\,\text{nm}$), 2 eV($\lambda = 620\,\text{nm}$), and 3 eV($\lambda = 413\,\text{nm}$). The curves are normalized such that the area under each is equal, corresponding to unity probability of an electron having energy $E_e > 0$. Note that the assumption of uniform energy distribution[4,11] would result in rectangular EDJDOS curves, which would be a reasonable approximation for the example shown here.

The shaded area under each curve in Fig. 2(a) shows the proportion of hot electrons with sufficient energy to be emitted over a Schottky barrier with $\Phi_B = 1.2\,\text{eV}$. This proportion is small when $\hbar\omega \sim \Phi_B$, and increases with increasing photon energy. The probability of a hot electron having $E_e > \Phi_B$ is given by

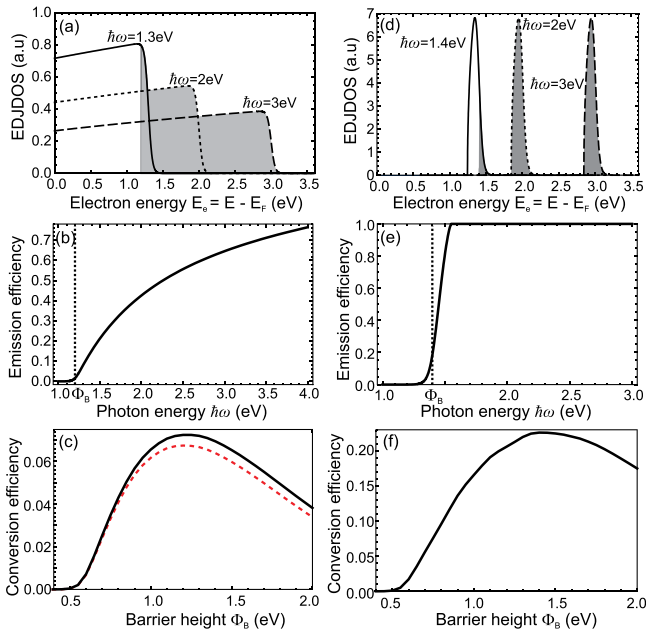

FIG. 2. (a) Distribution of hot electron energies (EDJDOS) in Ag for incident photons of energy $\hbar\omega$. Zero on the horizontal axis is E_F. Shaded areas indicate electrons with sufficient energy to cross a Schottky barrier of height $\Phi_B = 1.2\,\text{eV}$. (b) Electron emission efficiency (η_i) dependence on photon energy for the same parameters in (a). (c) Maximum power conversion efficiency as a function of Φ_B under solar illumination, calculated for the EDJDOS shown in (a) (solid) and for a uniform electron energy distribution (dashed). (d)-(f) show the same data as (a)-(c), but calculated for a narrow DOS distribution close to the Fermi level, and with $\Phi_B = 1.4\,\text{eV}$.

$$P(E_e > \Phi_B; \hbar\omega) = \frac{\int_{\Phi_B}^{\hbar\omega} \mathcal{D}(E, \hbar\omega) dE}{\int_{0}^{\hbar\omega} \mathcal{D}(E, \hbar\omega) dE}. \quad (4)$$

Figure 2(b) shows this probability calculated for $\Phi_B = 1.2\,\text{eV}$ as a function of the incident photon energy. Note that even when $\hbar\omega > 2\Phi_B$, only just over half (54%) of the excited electrons will have enough energy to pass over the barrier.

Hot electrons in the metal must travel ballistically to the junction before they can be emitted into the semiconductor and produce a photocurrent. The initial non-Fermi distribution of electrons illustrated in Fig. 2(a) has a lifetime of only a few hundred fs (~350 fs and ~500 fs for bulk Ag and Au, respectively)[17] before electron-electron collisions redistribute the energy to the surrounding electron gas. This thermalization results in a hot Fermi distribution of electron energies, which subsequently equilibrates with the atomic lattice through electron-phonon interactions on timescales on the order of 1 ps.[17] For efficient extraction, hot electrons must reach the junction before thermalization occurs. These timescales can be reformulated as a mean free path, ℓ_e, which can be relatively large for noble metals, with quoted values of ~50 nm for Ag, and ~40 nm for Au at energies close to the Fermi energy.[18] Thus, provided the metal layer is sufficiently thin, a large proportion of hot electrons will reach the Schottky barrier before losing energy through scattering processes.

When approaching the interface, an electron with $E_e > \Phi_B$ will only be emitted across the junction if the normal component of its momentum is sufficiently large to overcome the barrier. Thus, for a given electron energy, one can define an emission cone of angles relative to the interface such that electrons approaching from inside the cone will be emitted, while those outside the cone will be reflected back into the metal.[11] Assuming an isotropic distribution of electron directions in the metal, a significant fraction may be reflected back into the metal, even if their kinetic energy exceeds the barrier height. This effect is included in the modified Fowler emission equation which is commonly used to fit experimental photoemission curves.[5,7] However, if the thickness of the metal, t, is sufficiently small ($t \ll \ell_e$), electrons may pass through it multiple times and be reflected back to the interface, thereby increasing the emission probability.[11] This effect has been observed experimentally in spherical metal nanoparticles.[19] In the limit $\ell_e/t \to \infty$, the emission probability of an electron with energy $E_e > \Phi_B$ approaches unity.[11] We therefore assume here that all electrons with $E_e > \Phi_B$ will be emitted, consistent with a metallic absorber with characteristic dimensions $\ll l_e$. This corresponds to setting $\eta_i(\hbar\omega) = P(E_e > \Phi_B; \hbar\omega)$ in Eq. (4), in which case the curve in Fig. 2(b) is the IPCE.

We have identified the steps required to generate a photocurrent via plasmon enhanced IPE and discussed some of the factors that influence the IPCE. We now apply the results to calculate the maximum power conversion efficiency and discuss the consequences for PV applications. The numerical results are based on TiO_2, which is used in many IPE devices and dye-sensitized solar cells.[2,3,20,21] This choice does not significantly affect the results since the only material parameter in the calculations is the effective Richardson constant, A^*, which has a relatively weak contribution to the overall efficiency. The cell conversion efficiency is derived from the maximum power point of the current-voltage (I-V) response. Hence, we evaluate Eq. (2) for standard AM1.5G illumination using $\eta_{abs} = 1$, and η_i given by Eq. (4), and substitute this result into Eq. (1). The reverse current term in Eq. (1) is evaluated with $A^* = 6.71 \times 10^6\,\text{Am}^{-2}\,\text{K}^{-2}$, for TiO_2 (Ref. 22) and a temperature of 300 K. The barrier height, Φ_B, is taken as an independent variable that could be modified by the choice of metal/semiconductor materials or by including thin interface layers at the junction.

Figure 2(c) shows the power conversion efficiency as a function of Φ_B, calculated for the EDJDOS in Fig. 2(a). As expected, if the barrier height is small, the reverse (dark) current is large and the efficiency is low. As Φ_B increases, the reverse current decreases and the efficiency increases to a maximum 7.2% for $\Phi_B = 1.2\,\text{eV}$. Further increasing Φ_B reduces the forward current term (j_{sc}) as fewer of the incident photons have $\hbar\omega > \Phi_B$, and thus the efficiency drops again. The shaded areas in Fig. 2(a) and the dotted line in Fig. 2(b) correspond to the optimum barrier height. The dashed red curve in Fig. 2(c) shows the efficiency obtained when the electron energy distribution is assumed to be uniform in the range $0 < E_e < \hbar\omega$. In this case, the maximum efficiency of 6.2% also occurs for $\Phi_B = 1.2\,\text{eV}$.

The results in Figs. 2(a)–2(c) show that even with the optimistic assumptions used here, it is unlikely that IPE solar

cells based on metallic absorbers can achieve efficiencies beyond a few percent. We can, however, identify opportunities to increase the present limits. It is clear from Figs. 2(a) and 2(b) that the low efficiency is due to the electron DOS in the metallic absorber, which results in a broad distribution of hot electron energies (the EDJDOS). An ideal EDJDOS curve would have a narrow peak at $E_e = \hbar\omega$, corresponding to incident photons only exciting electrons from close to the Fermi level. Equation (3) shows two possible routes to achieve this. The first is to modify the electron DOS above the Fermi energy to suppress electron transitions to energies $E_e < \hbar\omega$. This is effectively the situation in a semiconductor absorber where the bandgap restricts the final energy of excited electrons to the levels in the conduction band.

The second way to modify the EDJDOS is to change the DOS of the occupied electron energy levels below the Fermi energy so that electrons close to E_F are excited preferentially over lower energy electrons. Experimental evidence suggests that this may already occur to some extent in noble metals. In Ref. 13, a small peak in the photoemission spectrum of Ag was attributed to a peak in the DOS 0.3 eV below E_F. Similarly, in Ref. 15, internal photoemission measurements of Ge/metal Schottky junctions were modeled by assuming a high DOS close to the Fermi level described by a parabolic DOS distribution with an effective conduction band edge just below E_F. While this is perhaps a somewhat unrealistic model, we use it here to illustrate how engineering the DOS in the absorber could increase the cell performance dramatically. Figures 2(d)–2(f) show the EDJDOS, electron emission efficiency, and power conversion efficiency calculated for an effective conduction band edge 0.15 eV below the Fermi level.[15] The narrow DOS distribution means that when $\hbar\omega > \Phi_B$, almost all of the hot electrons have sufficient energy to cross the barrier. As a result, the emission curve in Fig. 2(e) approximates a step-like function that goes from 0 when $\hbar\omega < \Phi_B$ to 1 for $\hbar\omega > \Phi_B$, and the maximum efficiency is 22.6% for $\Phi_B = 1.4$ eV (Fig. 2(f)). It may be possible to engineer the DOS in the absorber to approximate this idealized response using alloys,[23] or quantum confinement effects;[24] however, this would require extensive materials development. Such devices would have much in common with existing quantum dot[24] or dye-sensitized[20,21] solar cells.

In conclusion, we have shown that solar cells based on plasmon-enhanced IPE face severe efficiency limits due to the properties of metallic absorbers, with maximum theoretical efficiencies of ~7% predicted even with perfect optical absorption. The key to improving the efficiency lies in modifying the DOS of the absorber, but this may be difficult to achieve in practice. In the short term, plasmon-enhanced IPE may offer more benefits for Schottky junction photodetectors where increased optical absorption[25] is important for improved performance.

We acknowledge the Australian Research Council and the Australian Solar Institute for financial support.

[1]K. R. Catchpole and A. Polman, Opt. Express **16**, 21793 (2008).
[2]Y. Nishijima, K. Ueno, Y. Yokota, K. Murakoshi, and H. Misawa, J. Phys. Chem. Lett. **1**, 2031 (2010).
[3]Y. Takahashi and T. Tatsuma, Appl. Phys. Lett. **99**, 182110 (2011).
[4]F. Wang and N. A. Melosh, Nano Lett. **11**, 5426 (2011).
[5]M. W. Knight, H. Sobhani, P. Nordlander, and N. J. Halas, Science **332**, 702 (2011).
[6]A. Rogalski, Prog. Quantum Electron. **27**, 59 (2003).
[7]Y. K. Lee, C. H. Jung, J. Park, H. Seo, G. A. Somoraj, and J. Y. Park, Nano Lett. **11**, 4251 (2011).
[8]S. J. Fonash, *Solar Cell Device Physics*, 2nd ed. (Elsevier, Burlington, MA, USA, 2010).
[9]C. Sönnichsen, T. Franzl, T. Wilk, G. Von Plessen, J. Feldmann, O. Wilson, and P. Mulvaney, Phys. Rev. Lett. **88**, 077402 (2002).
[10]K. Aydin, V. E. Ferry, R. M. Briggs, and H. A. Atwater, Nature Commun. **2**, 517 (2011).
[11]C. Scales and P. Berini, IEEE J. Quantum Electron. **46**, 633 (2010).
[12]N. Smith, Phys. Rev. B **3**, 1862 (1971).
[13]C. N. Berglund and W. E. Spicer, Phys. Rev. **136**, A1044 (1964).
[14]R. Y. Koyama and N. V. Smith, Phys. Rev. B **2**, 3049 (1970).
[15]E. Chan, H. C. Card, and M. C. Teich, IEEE J. Quantum Electron. **QE-16**, 373 (1980).
[16]A. Kiejna and K. F. Wojciechowski, *Metal Surface Electron Physics* (Elsevier Science, Oxford, UK, 1996), Chap. 4, p. 57.
[17]C. Voisin, N. Del Fatti, D. Christofilos, and F. Vallée, J. Phys. Chem. B **105**, 2264 (2001).
[18]K. W. Frese, Jr. and C. Chen, J. Electrochem. Soc. **139**, 3234 (1992).
[19]Q. Y. Chen and C. W. Bates, Jr., Phys. Rev. Lett. **57**, 2737 (1986).
[20]E. McFarland and J. Tang, Nature **421**, 616 (2003).
[21]B. O'Regan and M. Grätzel, Nature **353**, 737 (1991).
[22]M. Ni, M. K. H. Leung, D. Y. C. Leung, and K. Sumathy, Sol. Energy Mater. Sol. Cells **90**, 2000 (2006).
[23]A. Slepko and A. A. Demkov, Phys. Rev. B **85**, 035311 (2012).
[24]P. V. Kamat, J. Phys. Chem. C **112**, 18737 (2008).
[25]S. R. J. Brueck, V. Diadiuk, T. Jones, and W. Lenth, Appl. Phys. Lett. **46**, 915 (1985).